DYNAMICS OF PERMANENT-MAGNET BIASED ACTIVE MAGNETIC BEARINGS

Satoru Fukata
Department of Energy and Mechanical Engineering, Kyushu University
Fukuoka 812-81, Japan.

Kazuyuki Yutani
Graduate Student, Kyushu University
Fukuoka 812-81, Japan.

SUMMARY

Active magnetic radial bearings are constructed with a combination of permanent magnets to provide bias forces and electromagnets to generate control forces for the reduction of cost and the operating energy consumption. Ring-shaped permanent magnets with axial magnetization are attached to a shaft and share their magnet stators with the electromagnets. The magnet cores are made of solid iron for simplicity. A simplified magnetic circuit of the combined magnet system is analyzed with linear circuit theory by approximating the characteristics of permanent magnets with a linear relation. A linearized dynamical model of the control force is presented with the first-order approximation of the effects of eddy currents. Frequency responses of the rotor motion to disturbance inputs and the motion for impulsive forces are tested in the non-rotating state. The frequency responses are compared with numerical results. The decay of rotor speed due to magnetic braking is examined. The experimental results and the presented linearized model are similar to those of the all-electromagnetic design.

INTRODUCTION

Active magnetic bearings that consist of permanent magnets giving bias flux and electromagnets generating control flux have been considered for the reduction of the high cost and the running energy consumption in the all-electromagnetic design. Reference 1 reviewed works related to this subject, but only a few reports are available to the authors. A key to this subject is the construction of magnetic circuits of the combined magnet system. Allaire et al.[1] discussed the design, construction and testing of a set that have permanent magnets in the stators. They also presented an analysis of the magnetic circuits. Their construction may be advantageous in use at high speeds. In addition, it is possible to combine a radial bearing with a thrust bearing.[1] However, because the permanent-magnetic bias-flux is not canceled out by the electromagnetic flux, the control force may be restricted.

This paper considers another construction in which the permanent magnets are attached to a shaft and their magnet stators are all shared with the electromagnets. This construction has a feature that it is possible to cancel out the bias flux with the electromagnetic flux. This point is a property similar to the all-electromagnetic design. However, since the composition of the rotor becomes complicated, there may be some problems to the rigidity of the shaft and to the elaborate machining of the rotor. This magnetic composition seems similar to an all electromagnetic case consisting of two independent magnet coils that are wound around the same poles and are assigned the separate functions of bias and control.

The magnet cores of the experimental setup are made of solid iron for simplicity of manufacturing. A simplified magnetic circuit of the combined magnet system is analyzed with the linear circuit theory by approximating the characteristics of permanent magnets with a linear relation. A linearized dynamical model of the control force is presented with a first-order approximation of the effects of eddy currents. The control systems are designed with simple analog PID compensators. Frequency responses of the rotor motion to disturbance inputs and the motion for impulsive force are tested in the non-rotating state. The decay of rotor speed due to magnetic brake is examined. The frequency responses are compared with numerical results.

PERMANENT-MAGNET BIASED RADIAL MAGNETIC BEARINGS

Figure 1 shows the mechanical part of the experimental setup of five-axis-control magnetic bearing system supporting a symmetric rotor in the horizontal direction. The radial bearings are composed of permanent magnets (ferrite) for biasing and electromagnets for control. The permanent magnet rings with axial magnetization are attached to a shaft of aluminum and are held between two iron rings each. The electromagnets are constructed with a pair of magnet coils that are wound around the stators positioned on the radially opposing sides: the pair of magnet coils are connected in series and are driven by a single power amplifier. The magnet poles in the vertical direction are one-fourth wider than those in the horizontal direction to supply larger bias flux for the suspension of the dead weight of the rotor. Four displacement sensors of the eddy current type are used to measure the radial motion of the rotor. The magnet cores are made of solid iron for simplicity of manufacturing. The rotor mass is 0.90kg, the airgap length is about 0.5 mm and the diameter of the rotor core is 40mm. The primary data are given later in Table 1.

A thrust bearing is positioned in the center of the setup using an electromagnet in place of the permanent magnet, for simplicity. Two magnet coils are wound around the inner core of the stator, one is for biasing and the other for control. The two opposing magnet coils on the left and right sides of the disc (the rotor of the thrust bearing) are connected in series to give similar magnetic circuits to the radial bearing. The rotor rotation is provided by compressed air blown onto teeth on the edge of the disc.

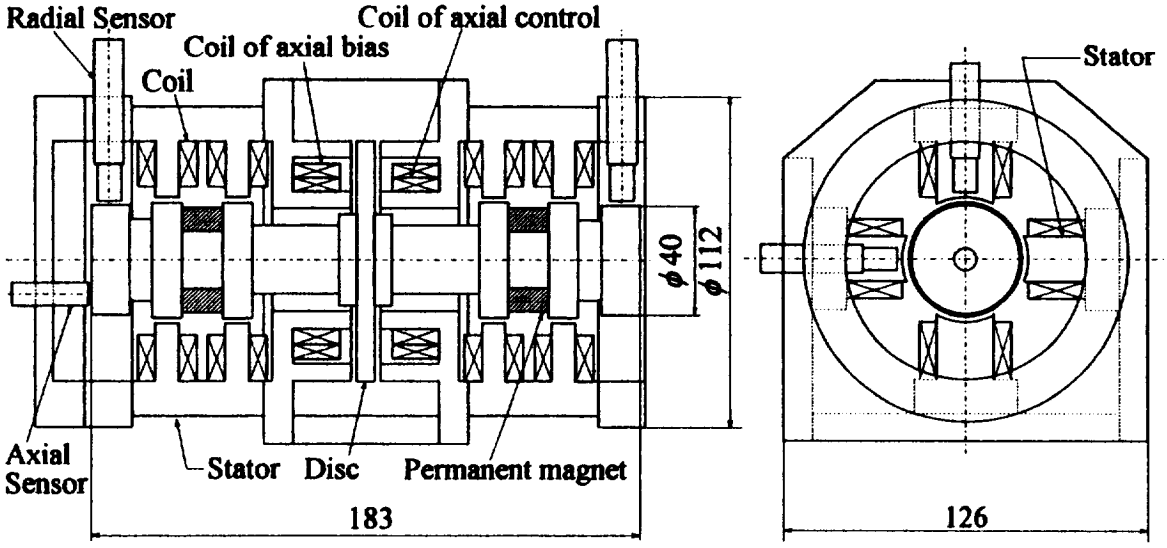

Figure 1. Construction of permanent-magnet biased magnetic bearing.

Figure 2 gives the magnetic flux paths of the radial bearing, neglecting leakage flux. The permanent magnetic flux, providing bias flux, flows radially in the iron-core ring and goes into the four poles of the stators through the airgaps, and passes through the stators along the axial direction to return to the rotor via the other airgaps. The electromagnetic flux generating from the upper and lower magnet coils passes down through the rotor along the radial direction on one side, and passes up through the other side. Thus, if the total flux increases in the lower side, then it decreases in the upper side. The difference of the flux produce a control force. With this construction, we can cancel out the bias flux with the electromagnetic flux. This is a point similar to the all-electromagnetic case. The configuration of the rotor, however, may be disadvantageous in use at high speeds, and there may be some problems in manufacturing the rotor.

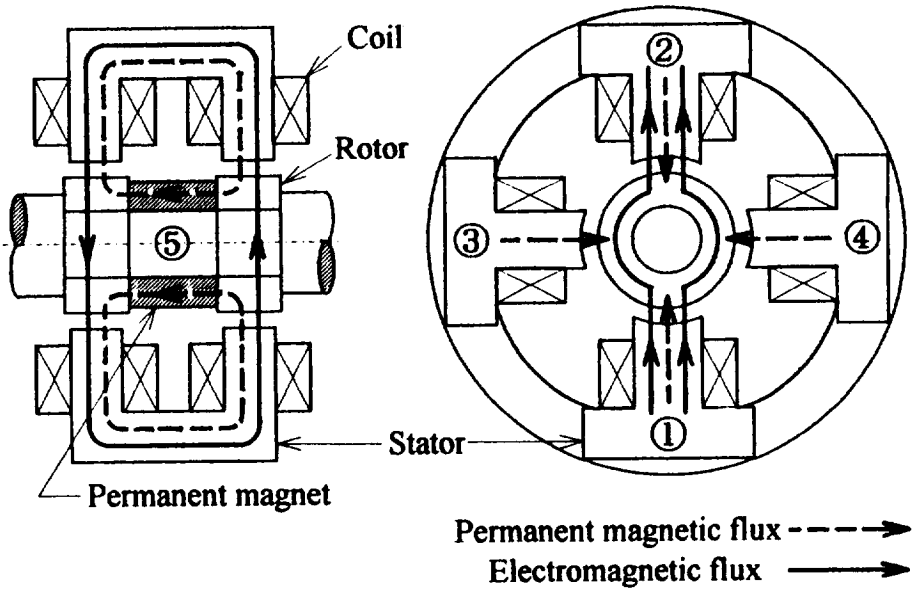

Figure 2. Magnetic flux paths of radial bearing.

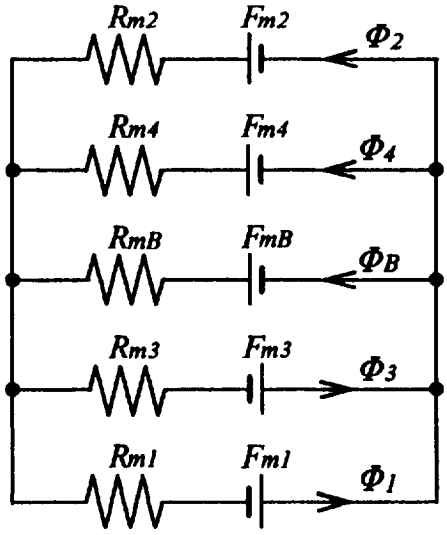

Figure 3. Simplified magnetic circuit.

ANALYSIS OF MAGNETIC SYSTEM

Magnetic Circuit of Radial Bearing

The characteristics of permanent magnets are considered based on the demagnetization curve. This curve may be quite linear for permanent magnets useful in practice such as ferrite magnets and rare-earth material magnets. Here, we approximate the demagnetization curve with a linear relation, using imaginary magnetomotive force and magnetic internal resistance. Then, as a model of the magnetic system of the radial bearing we consider the magnetic circuits in Fig. 3, where flux leakage is neglected. In the figure, F_{mj} is magnetomotive force, R_{mj} is magnetic resistance and Φ_j is magnetic flux associated with a stator numbered j in Fig. 2 and with the permanent magnet with B. The imaginary magnetomotive force F_{mB} and the magnetic internal resistance R_{mB} may be described as[2]

$$F_{mB} = l_m \frac{B_r}{\mu_r}, \qquad R_{mB} = \frac{l_m}{\mu_r A_m} \tag{1}$$

where B_r is the residual flux density, μ_r the recoil permeability, l_m the thickness and A_m is the area. For this circuit we have the following relations.

$$\begin{aligned} F_{m1} + F_{m2} &= R_{m1}\Phi_1 + R_{m2}\Phi_2 \\ F_{m1} - F_{m3} &= R_{m1}\Phi_1 - R_{m3}\Phi_3 \\ F_{m1} + F_{m4} &= R_{m1}\Phi_1 + R_{m4}\Phi_4 \\ F_{m1} + F_{mB} &= R_{m1}\Phi_1 + R_{mB}\Phi_B \\ \Phi_1 &= \Phi_2 - \Phi_3 + \Phi_4 + \Phi_B \end{aligned} \tag{2}$$

The magnetic resistances are estimated by

$$R_{mj} = \frac{2l_{mj}}{\mu_0 A_j} \tag{3}$$

where l_{mj} is an equivalent airgap length considering the magnetic path in the magnet core, μ_0 is the permeability of air, and A_j is the area of a magnet pole. Then, from eq. (2) we obtain the relations

$$\begin{aligned} R_{m1}\Phi_1 &= F_{m1} - \Delta F_{12} - \Delta F_{34} + \alpha_B F_{mB} \\ R_{m2}\Phi_2 &= F_{m2} + \Delta F_{12} + \Delta F_{34} - \alpha_B F_{mB} \\ R_{m3}\Phi_3 &= -\Delta F_{12} + F_{m3} - \Delta F_{34} + \alpha_B F_{mB} \\ R_{m4}\Phi_4 &= \Delta F_{12} + F_{m4} + \Delta F_{34} - \alpha_B F_{mB} \\ R_{mB}\Phi_B &= \Delta F_{12} + \Delta F_{34} + (1-\alpha_B) F_{mB} \end{aligned} \tag{4}$$

where

$$\Delta F_{12} = \alpha_1 F_{m1} - \alpha_2 F_{m2}, \qquad \Delta F_{34} = \alpha_3 F_{m3} - \alpha_4 F_{m4}$$

$$\alpha_j = \frac{R_T}{R_{mj}}, \quad j = 1 \sim 4, B; \qquad \frac{1}{R_T} = \sum_{j=1}^{4,B} \frac{1}{R_{mj}}$$

In the following, we take the center of the bearing as the nominal position of the rotor, and in place of the flux we use variables defined by

$$Q_j = \frac{R_{m10}}{N}\Phi_j, \quad j = 1,2; \qquad Q_j = \frac{R_{m30}}{N}\Phi_j, \quad j = 3,4 \tag{5}$$

where R_{mjo} are the nominal magnetic resistances, and N is the coil turns that are all the same here. The variables have the same dynamical characteristics as the flux and the unit of current, and give coil currents if the eddy-current effects are negligible. The variable was introduced first to simplify the description of electromagnet systems,[3] and effectively used in modeling the systems with eddy-current effects.[4] Then, we rewrite eq. (4) as follows:

$$\begin{aligned} c_{m1}Q_1 &= (1-\alpha_1)f_{m1} + \alpha_2 f_{m2} - \bar{f}_{34} + Q_B \\ c_{m2}Q_2 &= \alpha_1 f_{m1} + (1-\alpha_2)f_{m2} + \bar{f}_{34} - Q_B \\ c_{m3}Q_3 &= -\bar{f}_{12} + (1-\alpha_3)f_{m3} + \alpha_4 f_{m4} + Q_B \\ c_{m4}Q_4 &= \bar{f}_{12} + \alpha_3 f_{m3} + (1-\alpha_4)f_{m4} - Q_B \\ c_{mB}Q_B &= \bar{f}_{12} + \bar{f}_{34} + (1-\alpha_B)f_{mB} \end{aligned} \tag{6}$$

where

$$c_{mj} = \frac{R_{mj}}{R_{mj0}}, \quad f_{mj} = \frac{F_{mj}}{N}, \quad j = 1,2,3,4,B$$

$$Q_B = \alpha_B (F_{mB}/N)$$

$$\bar{f}_{12} = \alpha_1 f_{m1} - \alpha_2 f_{m2}, \quad \bar{f}_{34} = \alpha_3 f_{m3} - \alpha_4 f_{m4}$$

We refer the initial steady-state values with subscript 0. In the steady state without initial load in the horizontal direction, we have

$$\begin{aligned} &Q_{10} = I_{10} + Q_B, \quad Q_{20} = I_{10} - Q_B, \\ &Q_{30} = -Q_{40} = Q_B, \\ &f_{m10} = f_{m20} = I_{10}, \quad f_{m30} = f_{m40} = I_{30} = 0 \end{aligned} \tag{7}$$

In the following, we assume that
(1) The displacement of the rotor is sufficiently small.
(2) The incremental magnetic flux is sufficiently small.
We consider the increments

$$\begin{aligned} &q_j = Q_j - Q_{j0}, \quad \Delta f_{mj} = f_{mj} - f_{mj0}, \\ &\Delta\alpha_j = \alpha_j - \alpha_{j0} \end{aligned} \tag{8}$$

We write the magnetic resistance as

$$\begin{aligned} &R_{m1} = R_{m10}(1+k_{m1}), \quad R_{m2} = R_{m10}(1-k_{m1}), \\ &R_{m3} = R_{m30}(1+k_{m3}), \quad R_{m4} = R_{m30}(1-k_{m3}) \end{aligned} \tag{9}$$

where k_{mj} is the relative variation of the magnetic resistance. Then, the parallel magnetic resistance R_T defined under eq. (4), is expressed as

$$R_T \cong R_{T0}\left[1 - 2\left(\alpha_{10}k_{m1}^2 + \alpha_{30}k_{m3}^2\right)\right] \cong R_{T0} \tag{10}$$

where α_{10} and α_{30} are the nominal values. This implies that the parallel resistance is nearly constant under the assumption (1). This gives the increments of α_j as follows:

$$-\Delta\alpha_1 = \Delta\alpha_2 = \alpha_{T10}k_{m1}, \quad -\Delta\alpha_3 = \Delta\alpha_4 = \alpha_{30}k_{m3} \tag{11}$$

Substituting eq. (11) into the incremental equations of eq. (6), and neglecting the second-order terms of the increments, we obtain the following relations.

$$q_1 + Q_{10}' k_{m1} = (1-\alpha_{10})\Delta f_{m1} + \alpha_{10}\Delta f_{m2} - \alpha_{30}\Delta f_{m34},$$
$$q_2 + Q_{20}' k_{m1} = \alpha_{10}\Delta f_{m1} + (1-\alpha_{10})\Delta f_{m2} + \alpha_{30}\Delta f_{m34} \quad (12)$$
$$q_3 + Q_B k_{m3} = (1-\alpha_{30})\Delta f_{m3} + \alpha_{30}\Delta f_{m4} - \alpha_{10}\Delta f_{12},$$
$$q_4 + Q_B k_{m3} = \alpha_{30}\Delta f_{m3} + (1-\alpha_{30})\Delta f_{m4} + \alpha_{10}\Delta f_{12} \quad (13)$$

where

$$Q_{10}' = Q_{10} - 2\alpha_{10} I_{10} = (1-2\alpha_{10})I_{10} + Q_B,$$
$$Q_{20}' = -Q_{20} + 2\alpha_{10} I_{10} = -(1-2\alpha_{20})I_{10} + Q_B \quad (14)$$
$$\Delta f_{12} = \Delta f_{m12} - 2I_{10}k_{m1}, \quad \Delta f_{m12} = \Delta f_{m1} - \Delta f_{m2},$$
$$\Delta f_{m34} = f_{m3} - f_{m4} \quad (15)$$

Dynamical Linearized Equation of Incremental Flux

We discuss the vertical direction whose special case gives the results of the horizontal direction. We apply a model presented in Reference 3, considering the first-order effect of eddy currents. This model describes the electric and magnetic coupling system composed of the two stator-coils in series as

$$V_1 = R_{12} I_1 + N\left(\dot{\Phi}_1 + \dot{\Phi}_2\right) \quad (16)$$

$$\left(R_e i_e + L_e \dot{i}_e + N\dot{\Phi}\right)_j = 0, \quad \left(R_L i_L + N\dot{\Phi}\right)_j = 0, \quad j = 1,2 \quad (17)$$

$$F_{mj} / N = f_{mj} = I_1 + (i_e + i_L)_j, \quad j = 1,2 \quad (18)$$

where V_1, R_{12} and I_1 are the input voltage, resistance and current of the magnet coil; i_{ej} and i_{Lj} are the eddy currents in the magnet cores, R_{e1} ($= R_{e2}$) and R_{L1} ($= R_{L2}$) are the resistances, and L_{e1} ($= L_{e2}$) is the inductance of the equivalent eddy current loop; F_{mj} are the magnetomotive forces. Here, we take the coil current positive when it increases the flux in the stator 1 (in the lower side). For a power amplifier with output current control, we suppose that the input voltage is expressed as

$$V_1 = p(b' E_1 - I_1) \quad (19)$$

where E_1 is an input voltage to the amplifier, p is the control loop gain, and b' is a constant. In this case, eq. (16) is replaced by

$$pb' E_1 = (p + R_{12})I_1 + N\left(\dot{\Phi}_1 + \dot{\Phi}_2\right) \quad (20)$$

Using the variables defined by eq. (5) simplifies eqs. (17) and (19) as follows:

$$I_1 = b_1 E_1 - T_{R1}\left(\dot{Q}_1 + \dot{Q}_2\right) \quad (21)$$

$$\left(i_e + T_e \dot{i}_e\right)_j = -T_{0ej}\dot{Q}_j, \quad i_{Lj} = -T_{0Lj}\dot{Q}_j, \quad j = 1,2 \quad (22)$$

where

$$b_1 = \left(\frac{p}{p+R_{12}}b'\right)_1, \quad T_{R1} = \frac{L_{10}}{(p+R_{12})_1}, \quad L_{10} = \frac{N^2}{R_{m10}},$$

$$T_{0e1} = \frac{L_{10}}{R_{e1}}, \quad T_{0L1} = \frac{L_{10}}{R_{L1}}, \quad T_{e1} = \frac{L_{e1}}{R_{e1}} \tag{23}$$

Eliminating I_1, i_{ej} and i_{Lj} from eqs. (18), (21) and (22), we obtain the following equations.

$$\begin{aligned} T_{e1}\dot{f}_{m1} + f_{m1} &= b_1\left(T_{e1}\dot{E}_1 + E_1\right) - T_{21}\ddot{Q}_1 - T_{11}\dot{Q}_1 - T_{R1}\left(T_{e1}\ddot{Q}_2 + \dot{Q}_2\right), \\ T_{e1}\dot{f}_{m2} + f_{m2} &= b_1\left(T_{e1}\dot{E}_1 + E_1\right) - T_{21}\ddot{Q}_2 - T_{11}\dot{Q}_2 - T_{R1}\left(T_{e1}\ddot{Q}_1 + \dot{Q}_1\right) \end{aligned} \tag{24}$$

where

$$T_{21} = \left(T_R + T_{0L}\right)_1 T_{e1}, \qquad T_{11} = \left(T_R + T_{0L} + T_{0e}\right)_1$$

The interacting magnetomotive forces in eqs. (12) and (13), Δf_{m12} and Δf_{m34}, which are zero if there is no effect of eddy currents, make the analysis quite complicated. We suppose that these influences are secondary, and we will make a rough approximation. From the incremental relations of eq. (24), we have

$$\begin{aligned} T_{e1}\Delta\dot{f}_{m12} + \Delta f_{m12} &= -T_{0L1}T_{e1}\dddot{\bar{q}}_{12} - T_{0Le1}\ddot{\bar{q}}_{12}, \qquad \bar{q}_{12} = q_1 - q_2, \\ T_{0Le1} &= T_{0L1} + T_{0e1} \end{aligned} \tag{25}$$

This relation suggests that the interactions are dynamical, i.e. statically zero. On the other hand, eqs. (12) and (13) give the relations

$$\begin{aligned} \bar{q}_{12} &= -\bar{Q}_{12}'k_{m1} + (1-2\alpha_{10})\Delta f_{m12} - 2\alpha_{30}\Delta f_{m34}, \\ \bar{q}_{34} &= 4\alpha_{10}I_{10}k_{m1} + (1-2\alpha_{30})\Delta f_{m34} - 2\alpha_{10}\Delta f_{m12}, \qquad \bar{q}_{34} = q_3 - q_4 \end{aligned} \tag{26}$$

where

$$\bar{Q}_{12}' = Q_{10}' - Q_{20}' = 2(1-2\alpha_{10})I_{10}$$

Substituting eq. (26) into eq. (25) and a similar equation of Δf_{m34}, and taking the lowest derivative terms of the variables, we have the approximation

$$\begin{aligned} \Delta f_{m12} &= \bar{Q}_{12}'T_{0Le1}\dot{k}_{m1}, \\ \Delta f_{m34} &= -4\alpha_{10}I_{10}T_{0Le3}\dot{k}_{m1} \end{aligned} \tag{27}$$

We eliminate Δf_{m1} and Δf_{m2} from eq. (12) with (27) for Δf_{m34} and the incremental equations of eq. (24). Since the results have higher derivatives of k_{m1} and are so complicated, we neglect the higher derivatives than the first. Thus, we obtain the following results.

$$\begin{aligned} \tilde{T}_{21}\ddot{q}_1 + \tilde{T}_{11}\dot{q}_1 + q_1 + \left(\gamma_1 + Q_{10}'T_{e1}\right)\dot{k}_{m1} + Q_{10}'k_{m1} &= b_1\left(T_{e1}\dot{e}_1 + e_1\right), \\ \tilde{T}_{21}\ddot{q}_2 + \tilde{T}_{11}\dot{q}_2 + q_2 + \left(-\gamma_1 + Q_{20}'T_{e1}\right)\dot{k}_{m1} + Q_{20}'k_{m1} &= b_1\left(T_{e1}\dot{e}_1 + e_1\right) \end{aligned} \tag{28}$$

where

$$\begin{aligned} \tilde{T}_{21} &= \left(2T_{R1} + T_{0L1}\right)T_{e1}, \qquad \tilde{T}_{11} = 2T_{R1} + T_{0L1} + T_{0e1} + T_{e1}, \\ \gamma_1 &= 2I_{10}\left[(1-2\alpha_{10})T_{R1}' - 2\alpha_{10}\alpha_{30}T_{0Le3}\right], \qquad T_{R1}' = T_{R1} + \alpha_{10}(T_{0L1} + T_{0e1}) \end{aligned} \tag{29}$$

The time constants $\tilde{T}_{21}$ and $\tilde{T}_{11}$ are the same values that are given when we take the two opposing stator-coils to be one. This natural fact is easily confirmed with the definition of the time constants in eq. (23). Thus, the above results are similar to those of the all-electromagnetic cases,

except for the term with γ_1. This term appears without eddy current effect. We can see that its first term with T_{R1}' results from the effect of the opposite-side stator-coil system with a bias current. We note that this term is reduced by the second term that is due to the interaction from the horizontal direction.

Similar equations are derived for the horizontal direction, but it may be simpler to take another way. Adding the two equations of eq. (13) gives the equation without interaction to the summing variable as

$$2q_{30} + 2Q_B k_{m3} = \Delta f_{m3} + \Delta f_{m4}, \quad 2q_{30} = q_3 + q_4 \tag{30}$$

Then, using relations similar to the incremental form of eq. (24), we have

$$\tilde{T}_{23}\ddot{q}_{30} + \tilde{T}_{13}\dot{q}_{30} + q_{30} + Q_B\left(T_{e3}\dot{k}_{m3} + k_{m3}\right) = b_3\left(T_{e3}\dot{e}_3 + e_3\right) \tag{31}$$

In a similar way, the difference variable $\bar{q}_{34}$, with Δf_{m12} in eq. (27) we obtain the approximated equation

$$(1-2\alpha_{30})T_{0L3}T_{e3}\ddot{\bar{q}}_{34} + \left[(1-2\alpha_{30})T_{0Le3} + T_{e3}\right]\dot{\bar{q}}_{34} + \bar{q}_{34} = 4\alpha_{10}l_{10}\left\{\left[T_{e3} - (1-2\alpha_{10})T_{0Le1}\right]\dot{k}_{m1} + k_{m1}\right\} \tag{32}$$

Then, we have the expression of the decoupled form

$$q_3 = q_{30} + \bar{q}_{34}/2, \quad q_4 = q_{30} - \bar{q}_{34}/2 \tag{33}$$

Similar to the case in the vertical direction, the interaction due to the term Δf_{m12} reduces the effect of $\dot{k}_{m1}$.

The above results suggest that the interactions are primarily due to the bias current combined with the airgap variation in the biasing direction, and that this interaction into the horizontal direction becomes smaller at higher frequencies. The results become quite simple in the case of laminated magnet cores.

We will obtain the time constants in eqs. (28) and (31), experimentally, because it is difficult to estimate theoretically the time constants of the eddy current effects, defined in eq. (23). For the fixed airgap of the nominal length ($\dot{k}_{m1} = k_{m1} = 0$), we write eq. (28) with the parallel combination of two first-order time-lag systems, using the Laplace transforms, as

$$\frac{Q(s)}{bE(s)} = \frac{T_e s + 1}{\tilde{T}_2 s^2 + \tilde{T}_1 s + 1} = \frac{k_1}{T_1 s + 1} + \frac{1 - k_1}{T_2 s + 1} \tag{34}$$

where we omitted the subscript 1, and where

$$\tilde{T}_2 = T_1 T_2, \quad \tilde{T}_1 = T_1 + T_2, \quad T_e = (1-k_1)T_1 + k_1 T_2 \tag{35}$$

To give γ_1, the other time-constants, T_{0L1} and T_{0e1}, are calculated from these results and the theoretical value of T_{R1} with the relations in eqs. (29).

LINEARIZED EQUATIONS OF ROTOR MOTION

Linearized Equation of Control Force

The magnetic force acting between two pole faces with the magnetic flux Φ may be expressed as $F = (A_h / 2\mu_0)(\Phi / A)^2$, where A is the area of the pole face and A_h is its projected area on the plane perpendicular to the sense of the force. Applying this to the two poles with the same face area and using the variables of eq. (5), we have the resultant magnetic force acting on the rotor on the opposing sides as

$$F_{12} = c_{F1}\left(Q_1^{\,2} - Q_2^{\,2}\right), \qquad c_{F1} = \frac{\mu_0 A_h}{4}\left(\frac{N}{l_{m10}}\right)^2 \tag{36}$$

Then, the net force is given by

$$\Delta F_{12} = F_{12} - F_{120} = f_1 + c_{F_1}\left(q_1^{\,2} - q_2^{\,2}\right) \tag{37}$$

with the first-incremental force

$$f_1 = (k_{F1}/2)(q_1 + c_{Q1}q_2) \tag{38}$$

where

$$k_{F1} = 4c_{F1}Q_{10} = 4\frac{F_{10}}{Q_{10}}, \qquad c_{Q1} = \frac{-Q_{20}}{Q_{10}} \ (>0) \tag{39}$$

When the rotor approaches stator 1 with displacement z, the relative variation of the magnetic resistance, k_{m1}, may be approximated under the assumption (1) as

$$k_{m1} \cong -\frac{z}{l_{m10}} \tag{40}$$

Using eqs. (28) with this relation, and replacing $(q_1 + c_{Q1}q_2)/2$ by a new variable q_1, we write eq. (31) with the dynamical form as follows:

$$f_1 = k_{F1}q_1, \qquad \tilde{T}_{21}\ddot{q}_1 + \tilde{T}_{11}\dot{q}_1 + q_1 - a_{11}\dot{z} - a_{01}z = \beta_1 b_1\left(T_{e1}\dot{e}_1 + e_1\right) \tag{41}$$

where

$$\begin{aligned}
&a_{11} = a_{01}\left(\tilde{T}_{R1}' + T_{e1}\right), \qquad a_{01} = \frac{Q_{10}'}{2l_{m10}}\left(1 + c_{Q1}c_{Q1}'\right),\\
&\beta_1 = \frac{1}{2}\left(1 + c_{Q1}\right), \qquad c_{Q1}' = \frac{Q_{20}'}{Q_{10}'},\\
&\tilde{T}_{R1}' = \frac{(1 - c_{Q1})(1 - c_{Q1}')}{1 + c_{Q1}c_{Q1}'}\left(T_{R1}' - \tau_{0Le3}'\right), \qquad \tau_{0Le3}' = \frac{2\alpha_{10}}{1 - 2\alpha_{10}}\alpha_{30}T_{0Le3},
\end{aligned} \tag{42}$$

For the horizontal force, the result is directly obtained by application of eq. (31) to eq. (38) with $c_{Q1} = 1$ as follows:

$$f_3 = k_{F3}q_3, \qquad \tilde{T}_{23}\ddot{q}_3 + \tilde{T}_{13}\dot{q}_3 + q_3 - \frac{Q_B}{l_{m30}}\left(T_{e3}\dot{y} + y\right) = b_3\left(T_{e3}\dot{e}_3 + e_3\right) \tag{43}$$

where y is the displacement toward stator 3.

The above results are almost all the same as those of the all-electromagnetic case,[4] if we regard the equivalent bias flux Q_B as an equivalent bias current. The term with $\tilde{T}_{R1}'$ is inherent in the magnet system consisting of two opposing stator-coils with bias current. We see through the derivation that the interaction appears separately on each of the two opposing sides, but that their resultant effect becomes smaller, and is canceled out in the horizontal direction. In this way, our analysis may seem to be a waste of labor and space. The analysis, however, gives a deeper understanding of the phenomena, and shows the complexity of the magnetic system.

Linearized Equations of Rotor Motion

The radial position of the rotor is controlled by the resultant forces and resultant moments of the incremental forces in the two bearings. We number the bearings 1 and 2 on the left and right sides, respectively, and use these numbers in the subscript of the variables if necessary, for simplicity. We take the sense of the rotor displacement to be positive when going down, as in the above, and the sense of the conical motion to be positive when going down more in bearing 1 than in bearing 2. We rewrite the conical motions with the equivalent displacements at the bearing,[5] for convenience, and neglect the interactions due to the gyroscopic effects. Applying eq. (41) to the two radial bearings having the same characteristics and supporting a symmetric rotor, we obtain the linearized equations that are similar in form each other, for the rigid-rotor motion in the vertical direction, as follows:

Translatory motion:

$$m\ddot{z} = k_{F1}q_z + d_z,$$
$$\tilde{T}_{21}\ddot{q}_z + \tilde{T}_{11}\dot{q}_z + q_z - a_{11}\dot{z} - a_{01}z = \beta_1 b_1\left(T_{e1}\dot{e}_z + e_z\right) \tag{44}$$

Conical motion:

$$m_C\ddot{z}_C = k_{F1}q_{zC} + d_{zC},$$
$$\tilde{T}_{21}\ddot{q}_{zC} + \tilde{T}_{11}\dot{q}_{zC} + q_{zC} - a_{11}\dot{z}_C - a_{01}z_C = \beta_1 b_1\left(T_{e1}\dot{e}_{zC} + e_{zC}\right) \tag{45}$$

where d_z is disturbance force, and m_c and d_{zC} are the equivalent mass and force of the conical motion.[5] The control variables e_z and e_{zC} are related to the actual control inputs as

$$2e_z = e_{11} + e_{21}, \qquad 2e_{zC} = e_{11} - e_{21} \tag{46}$$

If the control variables are given, then the inputs, e_{11} on the left side and e_{21} on the right side, are determined by

$$e_{11} = e_z + e_{zC}, \qquad e_{21} = e_z - e_{zC} \tag{47}$$

Similar equations of the horizontal direction are obtained with $c_{Q1} = c_{Q1}' = 1$ in the above results.

EXPERIMENTAL AND NUMERICAL RESULTS

The primary data of the experimental setup are shown in Table 1. We mounted the setup by pressing on to a block of modelling clay. Experimental data are obtained in the non-rotating state except for the decay of rotation. We will show the results in the vertical direction; similar results are obtained in the horizontal direction.

Table 1 Data of Setup

Rotor		
Mass (PM contained)	$m = 0.90$	kg
Diameter	$D = 40.0\times10^{-3}$	m
Moment of inertia of conical motion	$J = 2.31\times10^{-3}$	kgm^2
Polar moment of inertia	$J_P = 3.51\times10^{-4}$	kgm^2
Distance between bearing centers	$l_1 = 111\times10^{-3}$	m
Distance between two gap-sensors	$l_2 = 174\times10^{-3}$	m
Stator (Radial)		
Magnet coil: Turns	$N = 200$	Turns
Resistance	$R = 0.62$	Ω
Area of pole face (Vertical)	$A_V = 1.60\times10^{-4}$	m^2
Area of pole face (Horizontal)	$A_H = 1.28\times10^{-4}$	m^2
Air gap length	$l_0 = 0.5\times10^{-3}$	m
Thrust bearing		
Bias coil : Turns	$N = 100$	Turns
Bias current	$I_0 = 1.0$	A
Control coil: Turns	$N = 100$	Turns

Magnetic Characteristics

It is difficult to theoretically estimate the time constants of our model. We examine the dynamical generation of the incremental flux by obtaining its frequency response to an input into the power amplifier. The generating voltage in a search coil gives the frequency response of the rate of the flux. We have the response of the flux by numerically multiplying $1/j\omega$ to this result represented in complex number, where j is the complex factor and ω is an angular frequency. The result measured with a 4-turn search coil is shown in Fig. 4 by the solid lines in the vertical direction, for the fixed airgap length of 0.5mm and the non-biasing input of the amplitude corresponding to the coil current of 0.38A statically. The phase in low frequencies is considered to be incorrect (the authors guess this is due to FFT analysis in the analyzer). The response has a characteristic that the phase lag in higher frequencies is small compared with the decay of the gain. We may understand this result with a first-order time-lag model in such a way that the increase in the magnetic resistance, due to the eddy current effects, decreases the incremental flux, but reduces the time constant that is inversely proportional to the resistance: the ratio of the inductance to the resistance.

To approximate the characteristics, we apply the model of eq. (34), and try curve fitting by selecting the two time constants and the weighting. The fitness depends on the range because of the low-order model. A result is shown in Fig. 4 by the broken lines; with this curve, we have T_1 = 0.17ms, T_2 = 1.88ms and k_1 = 0.40. The static gain of -84.4dB is given by the theoretical value

calculated with $b_1 = 0.36$ and l_{m0} = 1.05 x (airgap length) without flux leakage nor fringing effect. The lines zigzag through the experimental results, and may be unsatisfactory: the gain is larger in frequencies of about 15 to 100Hz, and the phase lag is smaller as a whole; however it seems difficult to have much more improvement. A similar result was obtained in the all-electromagnetic case.[6]

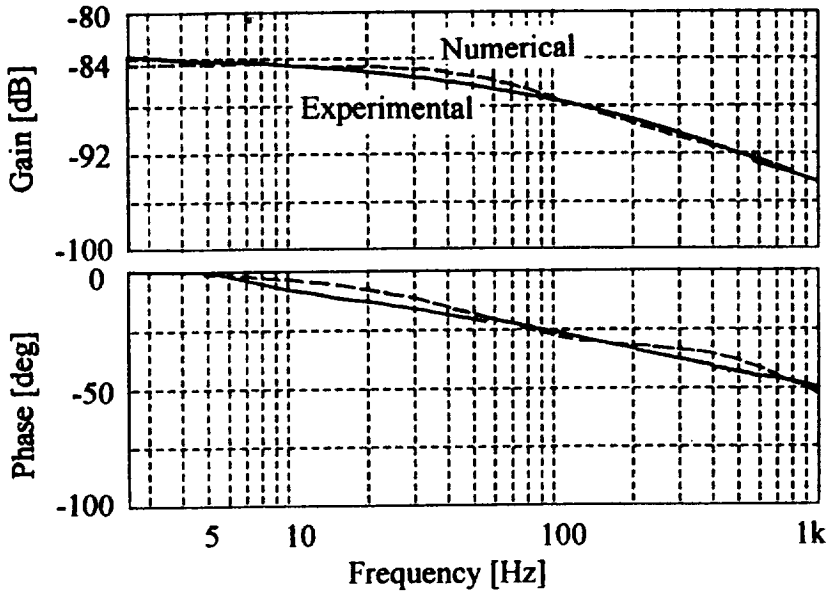

Figure 4. Frequency characteristics of incremental flux.

Control System

The control systems are constructed as in Fig. 5, for each of the vertical and horizontal motions, neglecting the interactions of the conical motions due to gyroscopic effects. This construction decouples the control of the translatory and conical motions into two single variable systems within the linearity. The input variables z_1 and z_2 are displacements of the rotor on the left and right sides. The outputs e_1 and e_2 are control inputs given to the electromagnet systems on the left and right sides. The variables z and z_c are displacements of the translatory and conical motions, u and u_c are control variables, and $C(s)$ and $C_c(s)$ are transfer functions of the compensators. The inputs u_0 and u_{0c} are used for the measurement of frequency responses of the control system. We used analog PID compensation.

Gains of the PID controllers were adjusted experimentally to give desirable characteristics of the control system. The selected gains gave the phase margin of about 35 deg. at 80~90Hz, and the gain margin of 15~18 dB at around 400Hz in the open-loop characteristics. The control inputs e_1 and e_2, including the bias input, are limited to a value corresponding to the static coil current of about 1.5A.

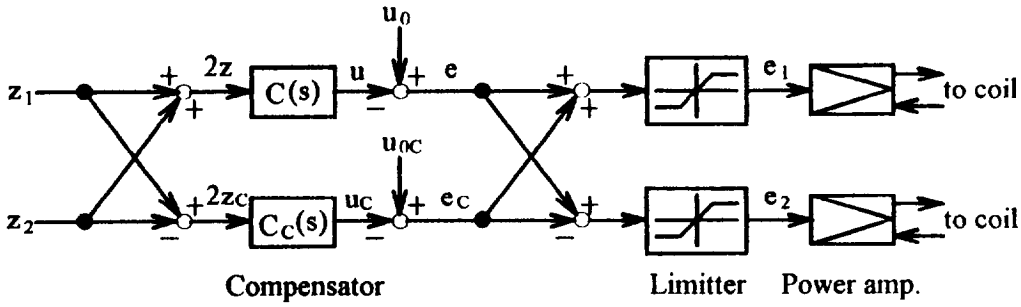

Figure 5. Control system.

Frequency Responses of Rotor Motion

Frequency responses of the rotor motion are measured for a sinusoidal input of amplitude 0.5V, corresponding to the coil current of about 0.19A statically. Figure 6 shows the responses of the vertical

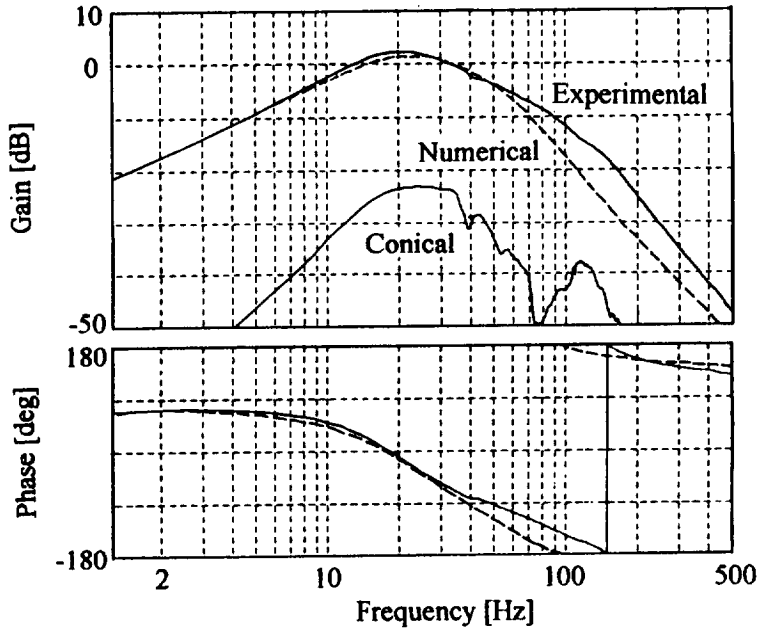

Figure 6. Frequency responses to translatory input.

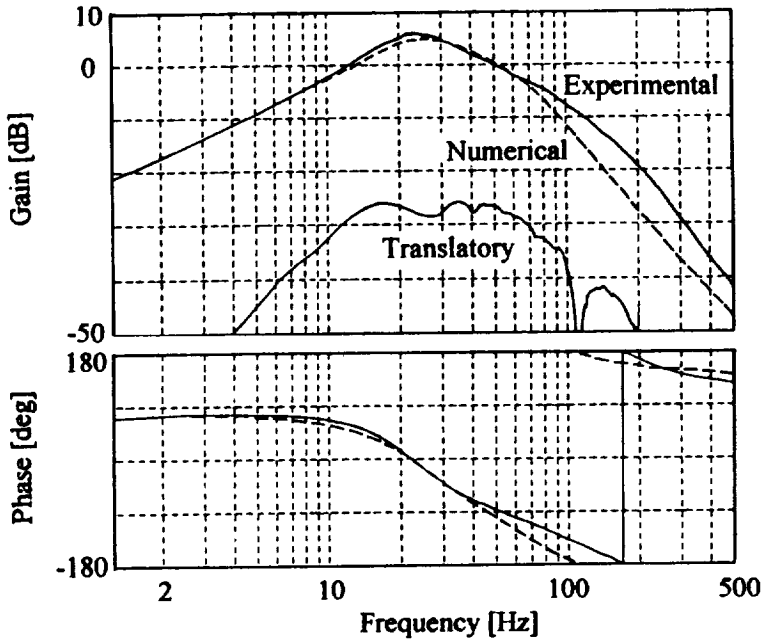

Figure 7. Frequency responses to conical input.

motion to the disturbance input of the translatory system. The phase is given only for the translatory motion. The maximum displacement in frequency about 20Hz is about 0.13mm, about one-fourth of the airgap length, (the output gains of the displacement sensor are 5.0×10^3 V/m for the translation, and 7.8×10^3 V/m for the conical motion). The induced conical motion is small as expected, but may have some information in higher frequencies. The responses to the input into the conical system are given in Fig. 7. The results are similar to the above results with a small translatory motion induced. The maximum displacement is about 0.13mm.

It was difficult to measure the permanent magnetic flux density in the airgap 0.5mm, therefore we guessed roughly 0.2T from the other measurement data. This flux density corresponds to an equivalent coil current of 0.84 A ($Q_B = 0.84$) and estimates the forces of 5.7N and 4.6N in the vertical and horizontal directions, respectively. In this case, the bias coil current in the vertical direction is calculated as 0.19 A ($I_{10} = -0.19$). The data necessary for the numerical analysis and the time constants obtained from the experiment, excluding data given in Table 1, are summarized in the followings.

$$b_1 \cong 0.36 \text{ A/V}, \quad p \cong 140 \text{ V/A}$$

$$\alpha_{10} = 0.25, \quad \alpha_{30} = 0.20, \quad \alpha_{TB} = 0.11, \quad R_{m10} = 5.0 \times 10^6 \text{ A/Wb}$$

$$T_{R1} = 0.057 \text{ ms}, \quad T_{0L1} = 0.26 \text{ ms}, \quad T_{0e1} = 0.82 \text{ ms}, \quad T_{e1} = 0.85 \text{ ms}$$

$$a_{01} = 2.11 \times 10^3 \text{ A/m}, \quad a_{11} = 1.83 \text{ As/m}, \quad c_{Q1} = 1.59, \quad c_{Q1}' = 1.26$$

We use T_{0Le1} in place of T_{0Le3} in eq. (42) because we have no data for it at present; however the authors suppose that this approximation is unimportant in this case.

The broken lines in Figs. 6 and 7 give the numerical results based on the linearized model. The results fit fairly well with the experimental results in lower frequencies, but poorly at frequencies higher than 150Hz. A further examination is required to explain this inconsistency. We guess at present that the primary cause is in the stiffness of the stators and in the supporting of the experimental setup.

Motion for Impact

Figure 8 gives the translatory motion and the actual control input for vertical impulsive force added at the center of the rotor for the maximum displacement of about 70% of the airgap. The shapes of the transient responses were similar for smaller motions, which is a result of the lower control gains.

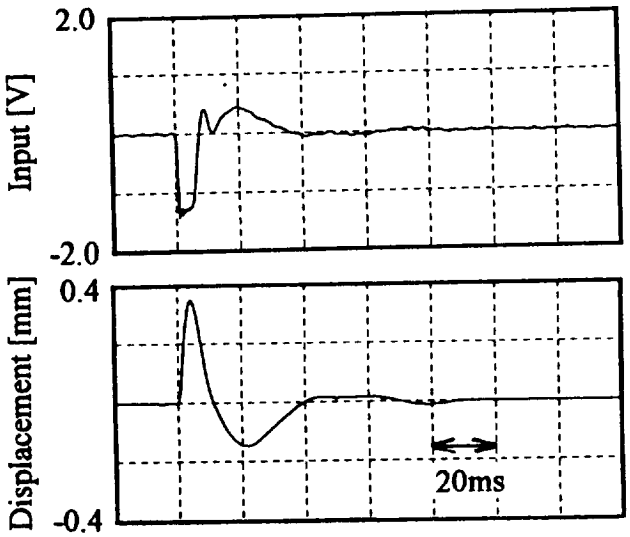

Figure 8. Translatory motion for vertical impact.

Decay of Rotation due to Magnetic Braking

We had a maximum rotating speed of a little more than 7,000 rpm, which was restricted by tolerable whirling of the rotor. The decay of the rotor speed starting from 7,000 rpm is observed as in Fig. 9. The rotor stopped completely after about 55s. A line connecting the points is approximated by the equation $\dot{\omega} + c\,\omega = -\tau_b$, $c = 0.046$ rad/s, $\tau_b = 72$ rad/s^2.

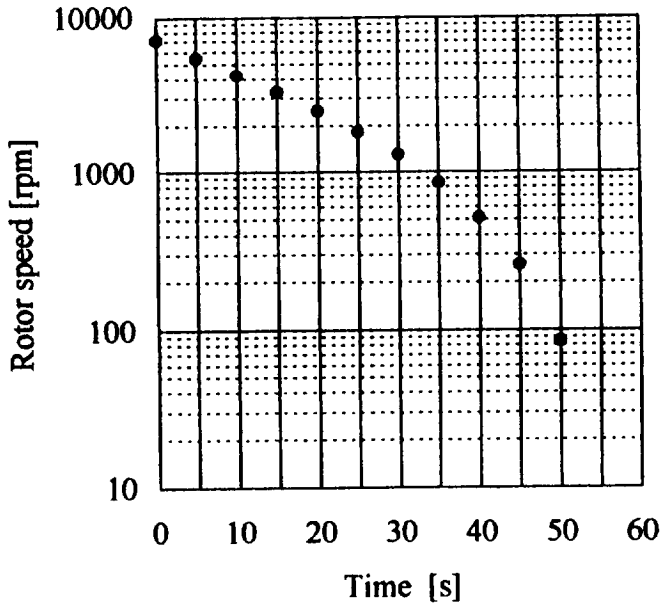

Figure 9. Decay of rotation.

CONCLUSIONS

Active magnetic radial bearings were considered with the combination of permanent magnets to give bias force and electromagnets to generate control force. The ring-shaped permanent magnets with axial magnetization are attached to a shaft and share all the magnetic poles with the electromagnets, so that the control flux may cancel out the bias flux. All the magnet cores are made of solid iron for simplicity of manufacturing. This, however, caused much complicated analysis. The simplified magnetic circuits were analyzed and the linearized dynamical model of control force was presented with the first-order effect of eddy currents. Frequency responses of the rotor motion to disturbance inputs and the motion for impulsive force are tested in the non-rotating state. The frequency responses are compared with the numerical results in some disagreement. The decay of rotor speed due to magnetic brake was examined. The experimental results and the presented linearized model are similar to those of the all-electromagnetic design.

We considered larger, but the same-size magnet poles in the vertical direction supporting the deadweight of the rotor, to reduce a decrease of the resultant bias force on the lower side. It may be reasonable to design different-size poles so that the permanent magnet may supply different bias fluxes to support a part or all of the initial load. In this case, however, the analysis of the magnetic circuits becomes much more complicated. Our approach may be a step towards this case.

The authors thank Mr. S. Fujino for help in making the experimental setup.

REFERENCES

1. Allaire, P.E.; *et al*: Permanent Magnet Biased Magnetic Bearings-Design, Construction, and Testing. *Proc. 2nd International Symposium Magnetic Bearings*, pp. 175-182, Tokyo, June 1990.

2. Ookawa, K.: *Introduction to Magnetic circuits of Permanent Magnets* (in Japanese), pp. 108-109, Sogo-Denshi Pub., Tokyo, 1994.

3. Fukata, S.; Kouya, Y.; and Tamura, H.: Dynamics of Active Magnetic Bearings, *Trans. Japan Soc. Mech. Eng.* (in Japanese), Vol. C-53, No. 490, pp. 1201-1207, 1987.

4. Fukata, S.: Linearized Model and Control Systems of Active Magnetic Bearings with Magnet Core in the Shape of a Cone. *Trans. Japan Soc. Mech. Eng.* (in Japanese), Vol. C-58, No. 551, pp.2081- 2088, 1992.

5. Fukata, S.; and Kouya, T.: Control Systems of Active Magnetic Bearings Based on Decoupling of the Motion of Rigid Rotor, *Technology Report of Kyushu Uni.*, Vol. 60, No. 2, pp. 185-191, 1987.

6. Fukata, S.; and Kouya, T.: Dynamics of Active Magnetic Bearings with Magnet Cores in the Shape of a Cone, *Proc. 3rd Inter. Sympo. Magnetic Bearings*, pp. 339-348, Alexandria, July 1992.